

# Coupling Solid Oxide Electrolyser (SOE) and ammonia production plant

**Giovanni Cinti<sup>1</sup>, Domenico Frattini<sup>2,4</sup>, Elio Jannelli<sup>2</sup>, Umberto Desideri<sup>3</sup>, Gianni Bidini<sup>1</sup>**

<sup>1</sup> *Università degli Studi di Perugia, via Duranti 93, 06125, Perugia Italy*

<sup>2</sup> *Università degli Studi di Napoli Parthenope, Centro Direzionale Napoli Isola C4, 80143 Naples, Italy*

<sup>3</sup> *Università degli Studi di Pisa, Largo Lucio Lazzarino, 56122, Pisa Italy*

<sup>4</sup> *Korea Institute of Science and Technology, Hwarangno 14-gil 5, Seongbuk-gu, 02792 Seoul, South Korea*

## Abstract

Ammonia is one of the most produced chemicals worldwide and currently is synthesized using nitrogen separated from air and hydrogen from natural gas reforming with consequent high consumption of fossil fuel and high emission of CO<sub>2</sub>. A renewable path for ammonia production is desirable considering also the potential development of ammonia as energy carrier. This study reports design and analysis of an innovative system for the production of green ammonia using electricity from renewable energy sources. This concept couples Solid Oxide Electrolysis (SOE), for the production of hydrogen, with an improved Haber Bosch Reactor (HBR), for ammonia synthesis. An air separator is also introduced to supply pure nitrogen. SOE operates with extremely high efficiency recovering high temperature heat from the Haber Bosch reactor. Aspen was used to develop a model to study the performance of the plant. Both the SOE and the HBR operate at 650°C. Ammonia production with zero emission of CO<sub>2</sub> can be obtained with a reduction of 40% of power input compared to equivalent plant.

**Keywords:** Sustainable Ammonia synthesis, Energy storage, Solid Oxide Electrolyser

## 1 Introduction

Ammonia production plays a significant role in the world emission of CO<sub>2</sub>. Ammonia is an intermediate chemical for the final production of all fertilizers based on urea that represents 78% of European fertilizers [1]. In addition, ammonia was presented recently as a potential fuel and as an eligible energy vector [2]. Such opportunity comes from ammonia high density in terms of energy content. Volumetric and gravimetric energy density of ammonia at room temperature and 10 bar are 22.5 MJ/kg and 13.6 GJ/m<sup>3</sup> respectively, higher than other candidates such as hydrogen and methanol and not far from fuels from fossil sources such as gasoline, diesel and compressed natural gas. The utilization of ammonia as a fuel was reported with interesting results in all traditional power units [3]. Ammonia combustion develops heat that can be used both in internal and external combustion engine [XX]. In addition, the use of ammonia as a fuel is also demonstrated in fuel cells with consequent advantages in terms of low emissions and high efficiency. Ammonia is a carbon free fuel, no CO<sub>2</sub> is emitted when burnt, and in fuel cell applications the risk of NO<sub>x</sub> production is reduced because no direct mix between oxygen and ammonia occurs. A sustainable use of ammonia both as chemical and as fuel requires a renewable production of NH<sub>3</sub> [4,5,XXX]. Ammonia is usually produced in the Haber Bosch (HB) loop reactor from pure hydrogen and nitrogen that are fed and recirculated in the reactor, operating at high pressure and high temperature. Hydrogen is usually produced from fossil sources, such as natural gas, in an autothermal steam methane reformer or from a steam methane reformer and while nitrogen is separated from air. Both hydrogen and nitrogen should be supplied using renewable energy as a primary source: such as biomass, wind or solar [6,7]. In particular, from water

41 electrolysis and air separation powered by renewable electricity it is possible to produce the so called green  
42 ammonia without any CO<sub>2</sub> emission[8].

43 This kind of plant can also be used in electric grids with a large penetration of intermittent renewable energy  
44 sources to store energy into a fuel that allows the physical and temporal separation, of energy supply and  
45 demand. The green ammonia plant allows to store directly the renewable electricity into a chemical with high  
46 energy density and easy to stock and to transport. This concept was recently presented and studied in literature  
47 [9]. Some recent publications have shown that carbon free ammonia can be obtained within a range of  
48 consumption of 10-12 kWh/kg NH<sub>3</sub> [9-11].

49 Recent development of Solid Oxide Fuel Cells (SOFCs) brought novel interest on high temperature Solid Oxide  
50 Electrolysers (SOEs), based on the same materials and design [12]. SOEs operate with high power density and  
51 efficiency than traditional electrolysers, especially if fed with high temperature waste heat, because the  
52 electrochemical conversion of water at high temperatures opens the opportunity to store both heat and  
53 electricity in the produced hydrogen [13]. Such opportunity is currently under study in industrial processes where  
54 waste heat recovery at high temperature is available. For example, the coupling is possible with nuclear power  
55 plants where heat is usually a by-product [14], or with solar collectors in solar thermal power plants, where  
56 renewable heat comes from the sun [13]. In this scenario, the coupling of SOE and HB process is extremely  
57 interesting. NH<sub>3</sub> synthesis is an exothermic chemical reaction at high temperature and pressure, thus in the  
58 energy balance of the plant, a large amount of heat is available. The integration between the HB process and the  
59 SOE potentially allows to transfer the heat produced by the HB reactor to the SOE to increase its performance.  
60 Moreover, the feasibility of ammonia production from renewable energy via electrolysis of water is of  
61 fundamental importance to produce sustainable fuels and chemicals.

62 This study proposes an improvement to green ammonia production plants introducing for the first time a SOE  
63 for H<sub>2</sub> production in a HB process. An electrochemical model and a thermodynamic simulation of a system layout,  
64 in which a SOE and an NH<sub>3</sub> plant are integrated and operated at high pressure and temperature, have been  
65 developed to evaluate the potential of the proposed concept with respect to other green solutions and to a  
66 reference benchmark case, based on the use of a fossil fuel. The effect on the global efficiency and on avoided  
67 CO<sub>2</sub> emissions is evaluated. This work can enhance the development of green ammonia and can offer, at the  
68 same time, an interesting application of SOE. In the following paragraphs the theory and modelling of SOE and  
69 HB process are presented, the design of the model is described and, finally, main results are analysed and  
70 commented.

## 71 72 2 Theoretical background and model development

### 73 2.1 Considerations for coupling and SOE electrochemical model

74 Ammonia synthesis is an exothermal process based on the following chemical reaction:



75 The distinctive features of this equilibrium reaction is that the contrasting effects of pressure and temperature  
76 limit its thermodynamics and kinetics, according to the following equations [15]:

$$K_{NH_3} = K_\phi \cdot K_p = \left( \frac{\varphi_{NH_3}}{\varphi_{N_2}^{1/2} \cdot \varphi_{H_2}^{3/2}} \right) \cdot \left( \frac{n_{NH_3}}{n_{N_2}^{1/2} \cdot n_{H_2}^{3/2}} \cdot \frac{n_{tot}}{P_{tot}} \right) \quad (ii)$$

$$r_{NH_3} = r_{dir} - r_{ind} = k_1 \cdot P_{N_2} \cdot \left( \frac{P_{H_2}^3}{P_{NH_3}^2} \right)^\alpha - k_2 \cdot \left( \frac{P_{NH_3}^2}{P_{H_2}^3} \right)^\beta \quad \alpha + \beta = 1; \quad \alpha, \beta > 0 \quad (iii)$$

77 The first is the chemical equilibrium constant in which non ideal fugacity coefficients are accounted in the term  
 78  $K_\phi$ . The term  $K_\phi$  account for the reactor operating conditions. The second is the so-called Temkin-Phyzev rate  
 79 equation for ammonia reaction kinetics. According to these two equations, an efficient and high conversion of  
 80 reactants in ammonia is favoured by:

- 81 • High pressure and temperature of the reactor.
- 82 • Stoichiometric  $H_2/N_2$  ratio in the reactor feeding stream.
- 83 • Absence of inerts or diluting species.

84 Ammonia synthesis is thus realized mainly with the plant design developed by Haber and Bosch (HB). The design  
 85 regards the number and the relative position of many functional units around the synthesis reactor, in order to  
 86 obtain an overall recycling loop. The fundamental units required to realize an HB plant are:

- 87 • A gas clean-up unit, to purify the raw syngas coming from upstream processes if any.
- 88 • A compression unit, to compress purified syngas to the HB reactor pressure.
- 89 • Heat exchanger and flash drum units for heat recovery and condensation of ammonia.
- 90 • Auxiliary streams for purging inert gasses out from loop and for recirculation of unconverted gasses.

91 The HB design is shown in Figure XX.

92

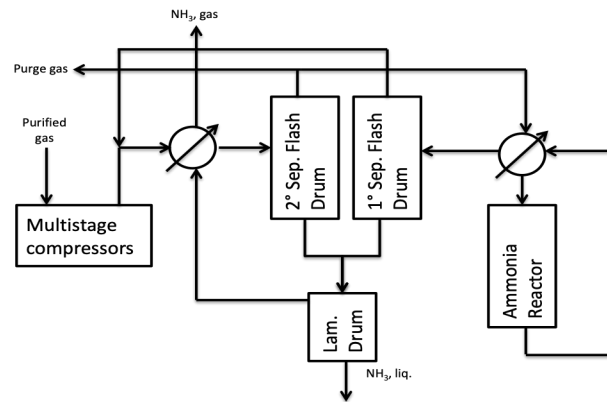


Figure 1 HB process layout for production of  $NH_3$

93  
94

95 The first two points determine the conversion per pass in the HB, according to thermodynamics and kinetics of  
 96 equations (ii) and (iii). The last two points mainly contribute to the global conversion and productivity of the  
 97 plant. Nevertheless, considering the presence of high and low temperature units, heat recovery issues arises and  
 98 they both influence the energy efficiency and the production of pure ammonia [16]. The HB process considered  
 99 in this work is based on a modern layout, to optimize the above mentioned parameters by coupling it with a SOE.  
 100 SOE conceptual scheme is depicted in Figure 2.

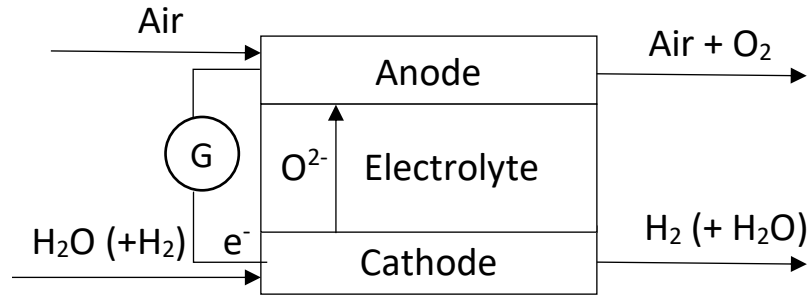
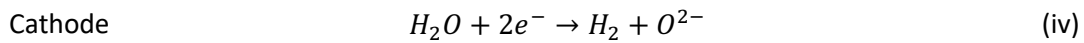
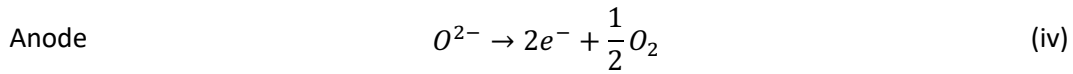


Figure 2 SOE conceptual scheme

101  
102

103

104 Anodic and cathodic reactions are:



105

106 The overall electrolysis reaction is the following:



107 The reaction is endothermic and the inlet energy, equal to  $\Delta H$ , has to be supplied externally. In the  
 108 electrochemical devices, like fuel cells, such energy is supplied as electrical ( $\Delta G$ ) and thermal energy ( $T\Delta S$ ).  
 109 Thermal energy is usually generated inside the cell, recovering heat from internal polarization losses. With the  
 110 increase of temperature, total energy requirement ( $\Delta H$ ) increases but the amount of electrical energy is smaller.  
 111 The results is a higher efficiency of the high temperature electrolyser than low temperature ones. If part of the  
 112 heat necessary is supplied by an external source, it is possible to achieve efficiency higher than one, obtaining  
 113 the conversion of thermal energy into chemicals.

114 Thermodynamic values at 650°C are reported in Table 1. Note that values are normalized for one mole of  $H_2$   
 115 produced (electrolysis) or reacting (ammonia synthesis).

116

	Temperature [°C]	Pressure [bar]	$\Delta H$ [kJ/mol $H_2$ ]	$T\Delta S$ [kJ/mol $H_2$ ]	$\Delta G$ [kJ/mol $H_2$ ]
Water electrolysis	650	1	-247.03	-49.57	197.46
Ammonia synthesis	550	250	35.76	37.75	-1.99

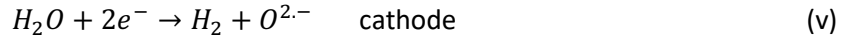
117

Table 1 Thermodynamic values of involved reactions

118 Ammonia synthesis can supply up to 73% (36.24 kJ/mol  $H_2$ ) of the heat required, in terms of entropy, of the  
 119 electrolysis reaction (49.57 kJ/mol  $H_2$ ). In order to couple thermodynamic and electrochemical calculations for  
 120 integration with the HB process, a zero dimension model for the SOE was developed as follows.

121 In a SOE, reaction (iv) is an electrochemical reaction which occurs in the electrolyser. The results are the two  
 122 reactions here below:

123



124  
125 Electrical inputs supplies the electron flows involved in the reactions. In electrolyzers, voltage is a function of  
126 current density and can be described with a very simple linear law as follows:

$$V = OCV + ASR(T) * J \quad (\text{vii})$$

127 Where OCV is the Open Circuit Voltage, ASR is Area Specific Resistance and J is current density. Both OCV and ASR  
128 are function of temperature. This simplified approach is supported by experimental results that show how the  
129 polarization curve is highly linear at high temperature [ref]. In additions authors already demonstrated how ASR  
130 does not change between SOFC and SOE operation [17]. This assumption will be used in defining values of ASR.  
131 In the following equation (iv) SOE electrical power density is described as follows:

$$P_e = V * J = OCVJ + ASR * J^2 \quad (\text{viii})$$

132 Energy output of the SOE is the energy of produced hydrogen. Such energy is the chemical energy of the fuel  
133 usually quantified in the LHV. For this study such energy was considered the enthalpy of the reaction (i)  
134 equivalent to the LHV of the fuel. Differently from LHV, the calculation was performed at the operative  
135 temperature. Specific chemical energy (in terms of energy flow per unit area) converted in the SOE is defined as  
136 follows:

$$\Delta H = dh(T) * H_{2mol} \quad (\text{ix})$$

137 Where  $H_{2mol}$  is the specific molar flow ( $\text{mol}/\text{m}^2$ ) of hydrogen and  $dh(T)$  is the enthalpy of the reaction (i). Hydrogen  
138 specific flow and current density are connected to the electrochemical parameters by the equation:

$$H_{2mol} = \frac{J}{2 * F} \quad (\text{x})$$

139 Where F is the Faraday constant. Differently from fuel cells, the reaction in electrolyzers is endothermal and the  
140 heat generated from process irreversibilities, such as current losses, are in equilibrium with reaction  
141 requirements. The energy balance is completed by the contribution of heat transfer with the external (Q). The  
142 latter takes into account the SOFC heat losses into the environment and the heat inlet from the environment  
143 that may come from a high temperature heat source, as in this application. External heat (Q) is calculated, for  
144 the present study, as a function of hydrogen energy production by the following equation

$$Q = k * \Delta H \quad (\text{xi})$$

145 The energy equilibrium of the SOE is defined by the following equation:

$$P_e = \Delta H + Q = \Delta H(1 + k) \quad (\text{xii})$$

146 Differently from fuel cells, were produced heat has to be subtracted by the air flow, in SOE the external heat  
147 contribution plays an importantrole not only on the operative temperature but also in the performances.  
148 Considering the stack at constant temperature, equation (viii) directly relates current density and temperature

149 to the external heat, in this case factor k. Thus, temperature definition and k allow to calculate the current  
 150 density. Considering the previous equations J can be calculated as:

$$J = \frac{1}{ASR} \left( \frac{dh(T) * (1 + k)}{2 * F} - OCV \right) \quad (xiii)$$

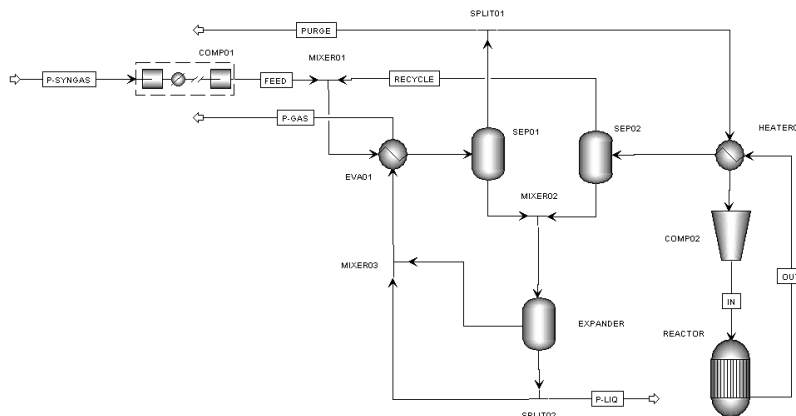
151 Efficiency is calculated as the ration between energy output ( $\Delta H$ ) and energy input ( $P_e$ ) by the following equation:

$$\eta = \frac{\Delta H}{P_e} = \frac{1}{1 + k} \quad (iiv)$$

152 Note that the efficiency is only a function of external heat contribution (k). In the specific case of k=0 the SOE  
 153 operates in adiabatic conditions (no heat exchange with the environment) with a 100% theoretical efficiency.  
 154 This operational condition is called thermoneutral. All equations were implemented in a zero-dimensional model  
 155 developed using Excel and FluidProp© as database for thermodynamic parameters. The OCV value was  
 156 calculated using the well-known Nernst equation considering as cathodic inlet a steam flow with 10% hydrogen  
 157 (necessary for the integrity of the electrode) and as anodic flow air. ASR values are derived from a SOFC  
 158 commercial product [17] due to the aforementioned equivalence with SOE ones.  
 159

## 160 2.2 Description of developed case studies

161 In order to assess the profitability of coupling SOE and HB process for the production of green ammonia, Process  
 162 Flow Diagrams (PFDs) were realized in the AspenPlus environment to compare different scenarios. In particular,  
 163 three case studies were developed: a reference case, named NG-REF-HB, with conventional  $NH_3$  production from  
 164 natural gas, a low temperature electrolysis case, named EL-PSA-HB, with  $H_2$  and  $N_2$  produced from commercial  
 165 electrolyser and Pressure Swing Adsorption (PSA) respectively, and finally the case of SOE and HB with heat  
 166 recovery from the HBR in which the low temperature electrolysis is replaced by the high temperature one. An  
 167 advanced HB flowsheet has been drawn using AspenPlus Suite, according to the scheme of Figure 3 below, and  
 168 is always the same for each case.  
 169



170  
 171 **Figure 3 Flowsheet of the HB loop developed in AspenPlus**

172 The description of the parameters used in AspenPlus is as follows. The “MCompr” block type was used with the  
 173 rigorous ASME method for efficiency, heat and power consumption calculation of the multistage compressor  
 174 unit COMPO01. Intercooling temperature after each stage and the final discharge pressure were specified for  
 175 this block. EVA01 is modelled with a “HeatX” block type and the cold stream outlet temperature is fixed in order  
 176 to exchange as much heat as possible. The specifications for the remaining blocks are summarized in Table 2.

Specification	HBR	SEP01	SEP02	EXPANDER
Temperature (°C)	550	0	20	-
Pressure (bar)	250	250	250	1
Heat Duty (kW)	-	-	-	0

Table 2 Block specifications for the HB loop

179 The rigorous “RGibbs” reactor block is used to model the HBR with the Aspen built-in PENG-ROB method for  
 180 physical and chemical equilibrium calculations. The vapour-liquid equilibrium flash drum model “Flash2” is the  
 181 block used for SEP01, SEP02 and EXPANDER. The splitting ratio, i.e. the amount of purge gas, of the block SPLIT01  
 182 is used as convergence variable for the PFD. In order to increase the ammonia recovery from HBR product stream,  
 183 the tail gas from EXPANDER and a part of the liquid ammonia produced are used to push the cooling of the  
 184 feeding stream in EVA01. The cold stream coming out from this block, i.e. P-GAS, is gaseous NH<sub>3</sub> with some traces  
 185 of inerts which can be still considered as useful product of the plant. The HB loop thus described produces  
 186 ammonia both in liquid and gaseous forms.

187 The complete PFD of the reference case, NG-REF-HB is shown in Figure 4.

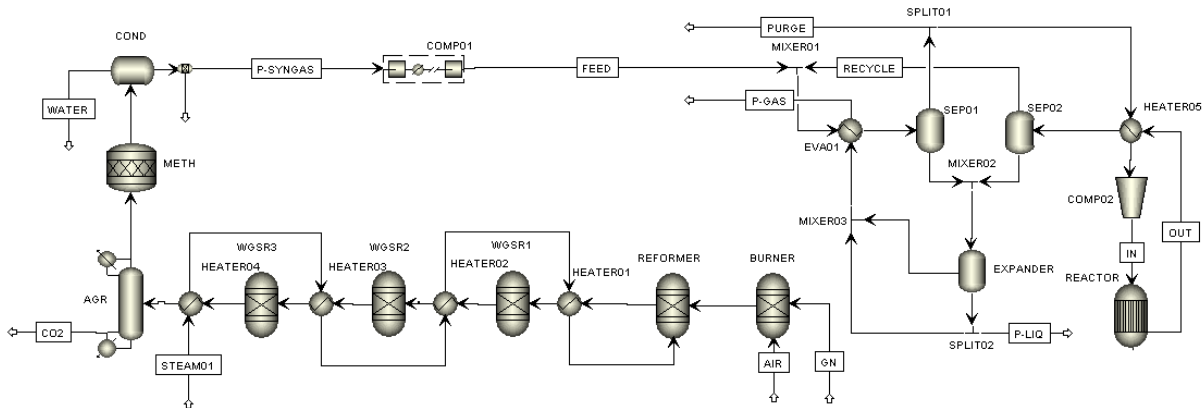


Figure 4 Flowsheet diagram of the reference case NG-REF-HB

191 Natural gas and air, at room temperature, are fed to an adiabatic combustor (BURNER), and a partial gasification  
 192 process occurs with H<sub>2</sub> and CO formed together with CO<sub>2</sub>. The N<sub>2</sub> necessary for NH<sub>3</sub> synthesis is fed in with the  
 193 AIR stream. In the block REFORMER, a pre-heated steam stream is added to the burnt gas. The Steam-to-Carbon  
 194 ratio (S/C) is fixed at 2 so that the Steam Methane Reforming (SMR) reaction can take place. Afterwards, three  
 195 reactors are used (WGSR1, WGSR2, WGSR3) to complete the Water Gas Shift reaction (WGS). The reactions  
 196 involved in these blocks are the following:

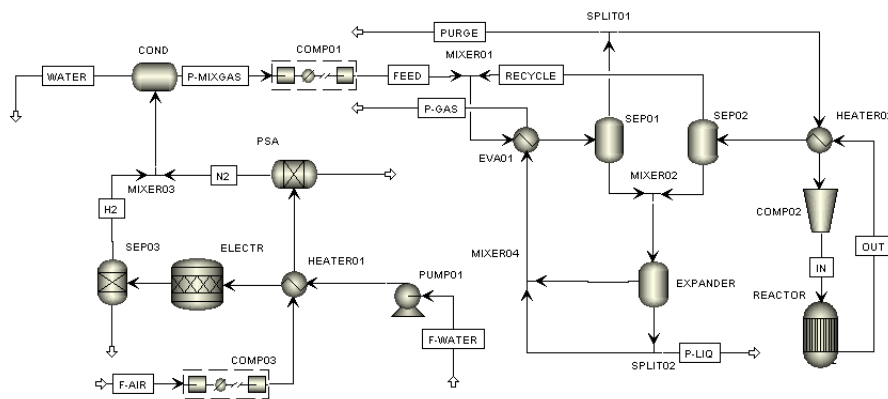


197 The reactor block used to model all these units is “RGibbs” and the built-in NRTL Aspen property method was  
 198 used for calculations. The Acid Gas Removal unit (AGR), the Methanator unit (METH) and the Condenser (COND)  
 199 are devoted to the physical and chemical separation and removal of CO<sub>2</sub>, CO and H<sub>2</sub>O after the WGS section. A  
 200 “Sep” block with standard specifications concerning temperature (≈50-80°C) and separation efficiency (>90%) is  
 201 used for the AGR block [18]. An adiabatic “RStoic” reactor block is used by METH to convert residual CO<sub>2</sub> and  
 202 COND is a “Flash2” block type, operated at 15°C to allow and complete gas/liquid separation. Table 3 summarizes  
 203 the specifications of those last three blocks.  
 204

Specification	AGR	METH	COND
Temperature (°C)	50	-	15
Pressure (bar)	1	1	1
Heat Duty (kW)	-	0	-

205 **Table 3 Block specifications for clean-up section**

206 The second case is named EL-PSA-HB and its schematic flow diagram is shown in Figure 5.  
 207



208 **Figure 5 Flowsheet diagram of the low temperature electrolysis case EL-PSA-HB**

210 The HB loop is the same as above, while the upstream architecture for low temperature electrolysis and PSA is  
 211 simpler: water is compressed in a hydraulic pump (PUMP01) and heated in a counter current heat exchanger  
 212 (HEATER01) to the electrolyser (ELECTR) operating conditions, namely 80°C and 30 bar. The built-in “Pump”  
 213 block has been used to model PUMP01, HEATER01 is a “HeatX” block type and ELECTR is an “RGibbs” reactor  
 214 block. The electrochemical calculations for ELECTR block are based on commercial alkaline electrolyzers data  
 215 from literature [19]. The PSA standard process was modelled in Aspen Plus by means of a compressor (COMP03)  
 216 and a separator (PSA) in series at 30 bar, room temperature and overall N<sub>2</sub> purity of 99.9% [20]. The property  
 217 method used in this section was the NRTL built-in Aspen model.  
 218 Finally, the last case is the SOE-PSA-HB process illustrated in the PFD of Figure 6.  
 219



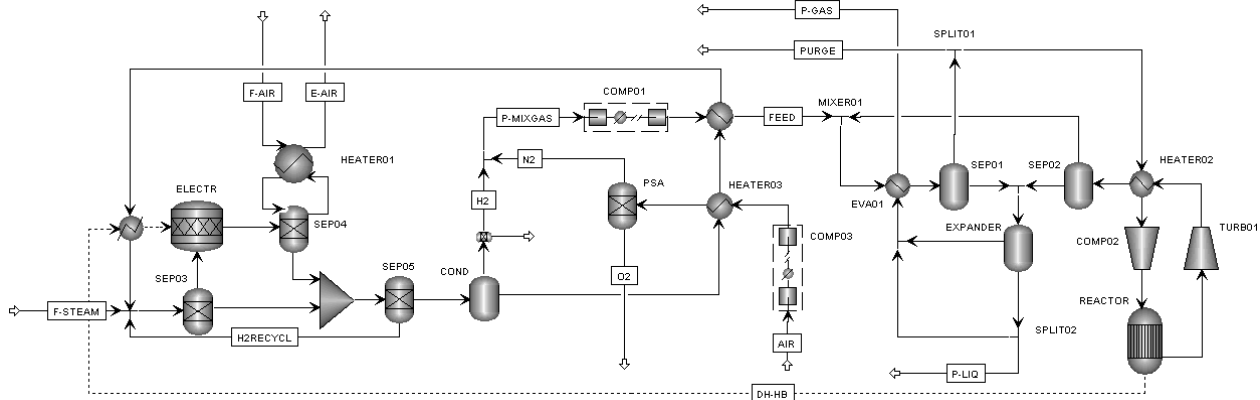


Figure 6 Flowsheet diagram of the high temperature electrolysis case SOE-PSA-HB

220  
221

222 In this case only, the ammonia reactor was forced to operate at 650°C and 550 bar. In order to have comparable  
 223 results with the previous cases, the different pressure level is controlled only in the HB REACTOR block by using  
 224 a pair of compressor/turbine before and after the block (COMP02, TURBO1). Selected temperature and pressure  
 225 are the highest that can be accepted for HB process and, at the same time, this temperature is the lowest possible  
 226 to consider in a SOE at the present stage of development. The upstream section, representing the SOE unit, was  
 227 adapted from a previous work [21] and slightly modified by just the addition of a condenser (COND) to separate  
 228 produced hydrogen (H<sub>2</sub>) from residual water, and a pre-heater at anode side (HEATER01), for preheating of the  
 229 sweeping air (F-AIR) by heat recovery from oxygen enriched air (E-AIR) coming from anode outlet. The water  
 230 separated from the COND block is used for cooling the feeding air of PSA block (AIR), and the feeding stream  
 231 (FEED) before the HB loop. Afterward, separated water is recycled to SOE as steam. Finally, the tear stream DH-  
 232 HB represents the chemical heat available from the REACTOR block, due to ammonia reaction according equation  
 233 (i), that is used in SOE. Similarly to the EL-PSA-HB case, an external subroutine was used for electrochemical  
 234 calculations, based on the model described in section 2.1, in order to consider the thermal contribution of HB  
 235 coupling to the SOE energy balance. The only inputs to the subroutine are the operational temperature, already  
 236 set at 650°C, and the heat supplied to the SOE (DH-HB) per unit of hydrogen produced, to calculate  $k$  used in  
 237 equation (xi).  
 238

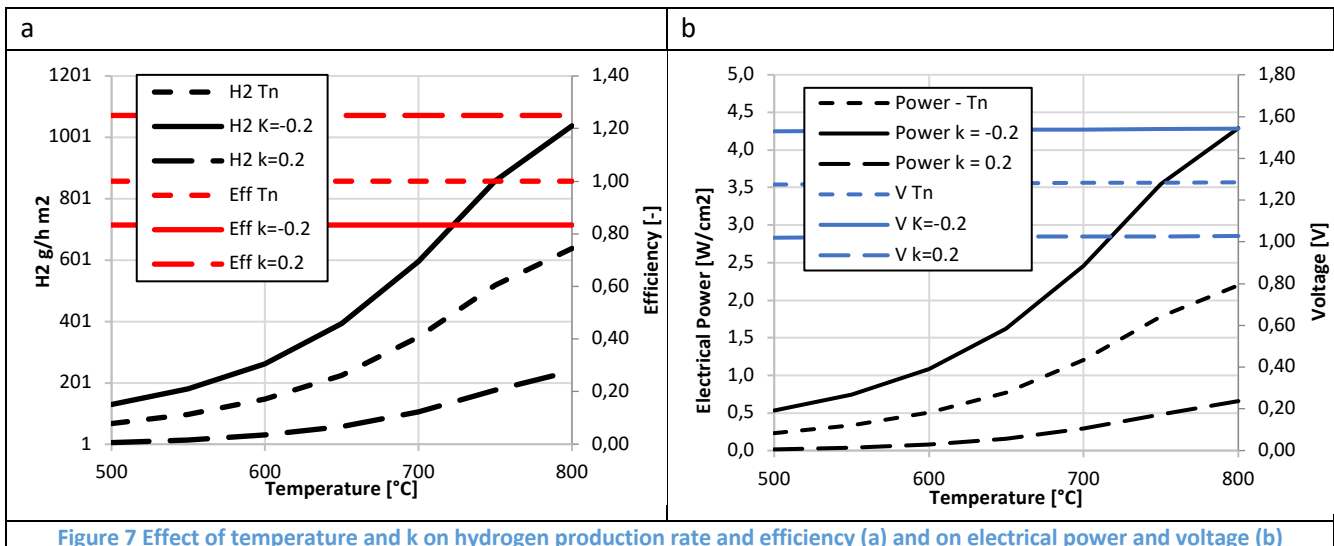


Figure 7 Effect of temperature and  $k$  on hydrogen production rate and efficiency (a) and on electrical power and voltage (b)

239

### 240 3 Results and discussion

241 Figure XX reports the variation of hydrogen production rate and efficiency (a) and of electrical power input and  
 242 voltage (b) as a function of temperature for three values of k: k=0 (thermoneutral), k=0.2 (heat into the SOE) and  
 243 k=-0.2 (heat losses). Figure 7 (a) shows a trade-off between efficiency and hydrogen production: with higher  
 244 values of k smaller efficiency can be obtained. As expected from equation (xiv), efficiency is not affected by  
 245 temperature variation while hydrogen production increases with temperature due to the decrease of internal  
 246 resistances (ASR). Regarding Figure 7 (b), Electrical Power density increases with temperature and is higher when  
 247 k is smaller (heat losses). Cell voltage remains constant at current density variation while increases when k  
 248 decreases. Thermoneutral voltage obtained is approximately 1.29 V in agreement with the literature [12].  
 249 Considering the coupling of ammonia synthesis with SOE, it is possible to calculate the k factor, considering the  
 250 heat flow from the ammonia reactor calculated from the Aspen model. At operational temperature of 650°C all  
 251 other SOE parameters are calculated and reported in Table 4.  
 252

Parameter	Units	Value
k	-	0.14
Temperature	°C	650
ASR	$\Omega \cdot \text{cm}^2$	0.57
OCV	V	0.94
H <sub>2</sub>	g/h·m <sup>2</sup>	108.18
J	A/cm <sup>2</sup>	0.29
Voltage	V	1.10
Power density	W/cm <sup>2</sup>	0.37
$\eta$	-	1.16

253 **Table 4 SOE parameter when integrated with NH<sub>3</sub> synthesis**

254  
255  
256  
257

The following Table 5 shows the major comparative parameters for the three scenarios. They refer only to the HB loop subsection of the flowsheet.

	(H <sub>2</sub> /N <sub>2</sub> ) <sub>FEED</sub> (mol/mol)	(H <sub>2</sub> /N <sub>2</sub> ) <sub>IN</sub> (mol/mol)	Rec. Ratio (mol/mol)	Purge Ratio (mol/mol)	$\eta_{\text{glob}}$ (%)	$\eta_{\text{react}}$ (%)
NG-REF-HB	3.07	3.17	3.33	0.44	61.12	18.25
EL-PSA-HB	3.01	3.02	4.29	0.08	92.33	21.06
SOE-PSA-HB	3.00	3.03	4.30	0.06	93.40	19.53

258 **Table 5 HB loop performances for the three different case studies**

259  
260  
261  
262

Comparing the values, remarkable differences are visible between the reference case, i.e. NG-REF-HB, and the remaining two, while the results obtained for the two cases with the use of electrolyzers seem to be very similar. The first two plants, the first fed with Natural Gas and the second based on a low temperature standard electrolyzer, can be operated at middle HB reactor conditions (250 atm and 550°C). SOE necessarily requires

263 heavy HB reactor conditions (550 atm and 650°C) for coupling, as discussed in section 2.1. Contrarily to what  
 264 could be expected, the conversion per pass and the global efficiency is very different for NG-REF-HB and EL-PSA-  
 265 HB, even if temperature and pressure of the HB reactor is the same. This is due to the high content of inert in  
 266 the reference case, i.e. CH<sub>4</sub>, that dilute the reactant steam and affect negatively the K<sub>p</sub> term as envisaged from  
 267 equation (ii). Moreover, the dilution of the products by the presence of CH<sub>4</sub> affects the physical separation of  
 268 ammonia because it reduces the partial pressure of NH<sub>3</sub> in SEP01 and SEP02 blocks. This is the cause of the low  
 269  $\eta_{\text{glob}}$  and the deviation of the H<sub>2</sub>/N<sub>2</sub> ratio inside the HB loop. As a consequence, the resulting purge ratio, i.e. the  
 270 purge gas stream, should be higher in order to avoid the accumulation of inerts in the loop. On the contrary, the  
 271 two cases with electrolyzers have very similar HB loop performances due to the complete absence of inerts. This  
 272 a distinguishing feature of ammonia production when electrolysis and air separation are used to provide the  
 273 H<sub>2</sub>/N<sub>2</sub> mixture. In particular, the purge ratio is very small, so that more reactant can be recycled to the reactor  
 274 instead of being purged with inerts. As a consequence, the recycle ratio, the NH<sub>3</sub> produced and the global  
 275 efficiency increase.

276 In Table 6 are reported the overall energy consumptions and the equivalent Green House Gas (GHG) emissions  
 277 of the three cases. They are normalized on the total quantity of ammonia produced. As reference, positive values  
 278 are intended as energy provided to the system, while negative values represent energy that should be subtracted  
 279 from the system.

280

	Spec. Chemical consumption (kWh/kg <sub>NH<sub>3</sub></sub> )	Spec. Electric consumption (kWh <sub>el</sub> /kg <sub>NH<sub>3</sub></sub> )	Spec. Total consumption (kWh/kg <sub>NH<sub>3</sub></sub> )	Spec. Heat consumption (kWh <sub>th</sub> /kg <sub>NH<sub>3</sub></sub> )	LHV of purge gas (MJ/kg)	GHG emissions (kg <sub>CO<sub>2</sub></sub> /kg <sub>NH<sub>3</sub></sub> )
NG-REF-HB	12.81	1.77	14.59	-1.20	26.76	2.05
EL-PSA-HB	0	14.25	14.25	-1.63	21.35	0
SOE-PSA-HB	0	8.30	8.30	-1.14	21.43	0

281

Table 6 Energy performances for the three different case studies

282 The first evident results is that for the case EL-PSA-HB and SOE-PSA-HB the specific chemical consumption is zero:  
 283 these systems are fed only by air and water so that there is no energy cost. On the contrary, the NG-REF-HB uses  
 284 a fuel, i.e. CH<sub>4</sub>, as feedstock. As expected, only the first case has a net environmental impact in terms of GHG  
 285 emissions due to the CO<sub>2</sub> release during the reforming and clean-up operations of the fuel. This is mainly  
 286 concentrated in the AGR block because it is one of the units devoted to the removal of oxygenated species from  
 287 the syngas for NH<sub>3</sub> synthesis. The remaining two cases have no net emissions because their feedstock is “carbon-  
 288 free”. The contribution to emissions, due to the carbon contained in the purge gas of the NG-REF-HB, is not  
 289 considered because, as shown in the table, the LHV of this stream is of interest in order to be used as a secondary  
 290 fuel or as a chemical feedstock. Moreover, keeping in mind the previous purge ratios and global efficiencies, it  
 291 could be concluded that the quantity of purge gas produced is considerable in the first system but negligible in  
 292 the last two. Finally, a significant difference on the total and heat consumptions occur for all cases. In particular,  
 293 even though the HB loop performances are quite the same, the cases with electrolyzer have very different  
 294 consumptions. Comparing the reference case and the standard electrolyzer case, it is worth to observe that the  
 295 total consumption is not so different, so that there is a little benefit in preferring the electrolysis pathway, power-  
 296 intensive but low impacting, rather than the traditional one, based on fossil fuel and less electricity-consuming  
 297 with the perspective to produce a valuable tail gas. However, the results show that in the case of coupling SOE,

298 PSA and HB, the total energy consumption can be potentially lower than all other solutions proposed.  
 299 To better understand this, in Figure 9 the detailed consumption of heat is specified for the main ancillaries of the  
 300 three developed scenarios. For the reference case, which has many ancillaries if compared to the other cases,  
 301 there is a considerable endothermic term, due to the heat required by the reformer block, and a high exothermic  
 302 contribution from the compression units, due to the interrefrigerations.  
 303

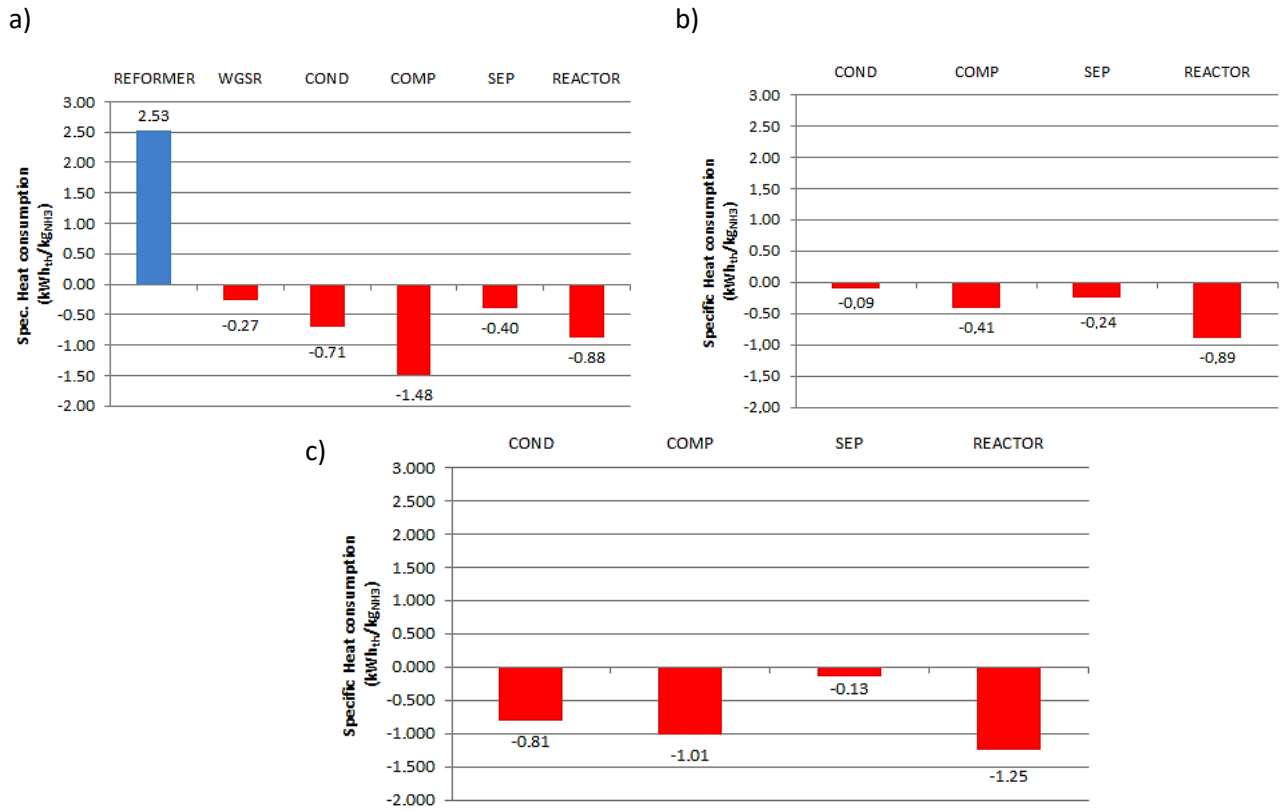
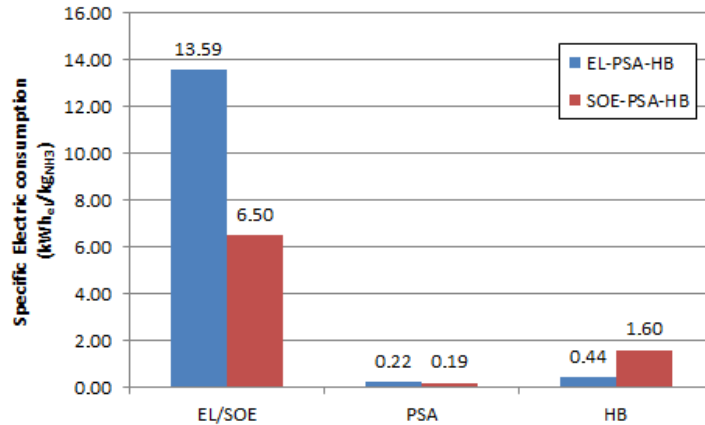


Figure 8 Specific heat consumption of ancillaries:

a) NG-REF-HB; b) EL-PSA-HB; c) SOE-PSA-HB.

304  
 305  
 306 The other two cases have smaller contributions, due to the simpler layout with no fuel thermal treatments or  
 307 gas clean-up units. Comparing Figure 9a and 9b, the heat available from HB reactor is the same because the  
 308 operating conditions are the same but, due to the presence of a high amount of inerts, the heat that should be  
 309 removed from hot streams is higher. The presence of species other than H<sub>2</sub>, N<sub>2</sub> and NH<sub>3</sub> in the HB loop is a strong  
 310 limit for productivity but also energy efficiency of traditional HB plant because, if compared to the contribution  
 311 of an electrolysis-based plant, they cause lower conversions and high waste heat. From this point of view, the  
 312 SOE-PSA-HB offers more flexibility and opportunity for a convenient recovery of waste heat. In Figure 9c not all  
 313 the contributions reported are really lost because, the heat from COND and REACTOR are used to achieve the  
 314 thermal equilibrium of the SOE block because this acts as a “heat sink” for the system. In detail the heat from  
 315 REACTOR is entirely used to feed SOE and is an input for the design of the electrolyzer. An additional advantage  
 316 of this configuration is that no cooling of ammonia reactor is required reducing the environmental impact in  
 317 terms of plant heat waste. One of the actual issue for SOE is that it requires a large amount of heat, or a high  
 318 current density, from external sources to sustain the high temperature electrolysis process. If SOE and HB loop  
 319 can be operated at similar temperatures, their coupling offer the opportunity to recover the large amount of

320 heat available from HB reactor to achieve a stable thermal equilibrium in the SOE, without increasing the current  
 321 density, i.e. the electricity consumption, as explained in the model above. The single contributions of COND and  
 322 REACTOR in the SOE-PSA-HB case are reported for completeness and to show how they become of interest if  
 323 compared to that of the mild HB reactor conditions.  
 324 The direct consequence of this fact can be immediately realized if the single electric consumptions are compared  
 325 as shown in Figure 10:

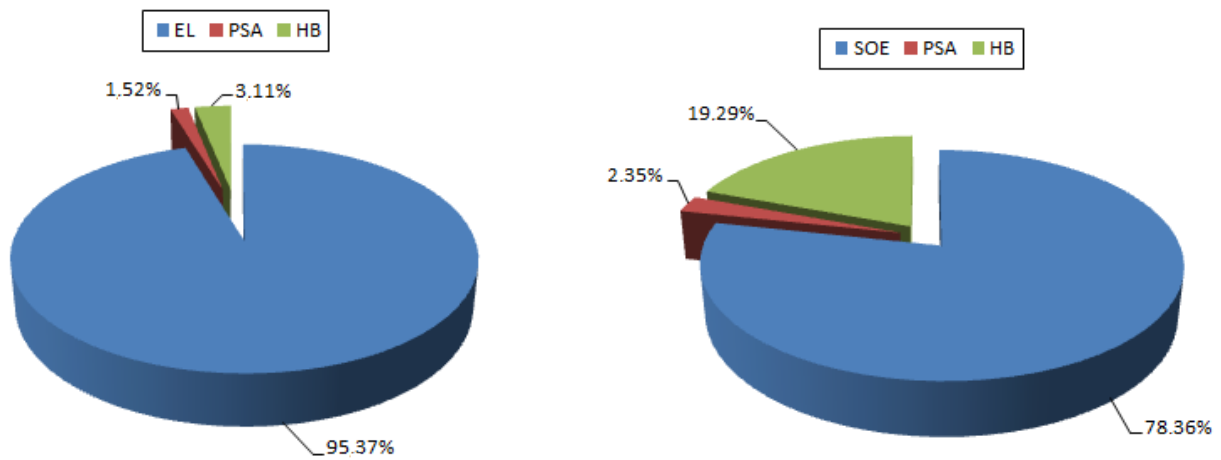


326  
327 **Figure 9 Comparison of the electric consumption for EL-PSA-HB and SOE-PSA-HB cases**

328 The first two columns clearly indicates the advantage of the high temperature electrolysis over the low  
 329 temperature one, if additional heat is provided from another source. The consumptions related to the PSA  
 330 subsection are the same for both cases, as expected, while the electric consumptions related to the compression  
 331 units of the HB loop are very different, essentially due to the high pressure imposed at the REACTOR block of the  
 332 SOE-PSA-HB. It is worth noting that for the reference case the electric consumption is represented only by the  
 333 compression units in the HB loop, and that its value is 1.77 kWh/kg<sub>NH3</sub>, the highest among the three scenarios,  
 334 because a large part of this energy is used to compress inerts which dilutes the syngas stream.  
 335 The coupling of SOE and HB deeply affects the energy balance of the plant when the electrolysis is used in place  
 336 of the reforming of a fossil fuel. Moreover, the type of electrolysis process modifies the distribution of energy  
 337 consumption within the plant itself. The situation is briefly explained in Figure 11.

a)

b)



338 **Figure 10 Distribution of the specific electric consumption:**

339 a) EL-PSA-HB; b) SOE-PSA-HB.

340 When a low temperature electrolysis is used to produce the syngas for the HB loop, the electric consumption  
341 related to the electrolyzer operation is >95% of the total, i.e. the overall energy balance is in practice restricted  
342 to the electrolyzer, so that there is no flexibility and the whole plant is dependent from the electrolysis  
343 subsection. On the other hand, when a SOE is implemented, its impact on the overall energy balance is lower, as  
344 shown in Figure 11: the share for the electrolysis subsection decreases from 95.37% to 78.36%.  
345

## 346 4 Conclusions

347 A novel system for the production of green ammonia was designed and analysed. The introduction of high  
348 temperature electrolyzer, such as SOE, permits to increase efficiency and system integration. The high efficiency  
349 of SOE permits electrical input reduction of the electrolyzer unit and to recover heat produced in the Haber Bosh  
350 reactor. The electricity consumption is decreased down to 14,25 kWh/Kg NH<sub>3</sub> and zero emission of CO<sub>2</sub> is  
351 obtained. In the field of chemical production the new system permits the production of zero emission ammonia  
352 and increase the flexibility of the plan compared to traditional electrolyzer. Considering also the use of ammonia  
353 as a fuel and the energy storage application, an high efficiency and high flexible concept is developed. Renewable  
354 electrical energy can be stored into a liquid vector that can be transported and directly used both for power and  
355 transport application.  
356

## 357 5 References

- 358 [1] Tallaksen, J., Bauer, F., Hulteberg, C., Reese, M., & Ahlgren, S. (2015). Nitrogen fertilizers manufactured  
359 using wind power: greenhouse gas and energy balance of community-scale ammonia production. *Journal of*  
360 *Cleaner Production*, 107, 626-635.
- 361 [2] NH3 as a fuel website
- 362 [3] Zamfirescu, C., & Dincer, I. (2009). Ammonia as a green fuel and hydrogen source for vehicular  
363 applications. *Fuel processing technology*, 90(5), 729-737.
- 364 [4] Zamfirescu, C., & Dincer, I. (2008). Using ammonia as a sustainable fuel. *Journal of Power*  
365 *Sources*, 185(1), 459-465.
- 366 [5] Esteves, N. B., Sigal, A., Leiva, E. P. M., Rodríguez, C. R., Cavalcante, F. S. A., & de Lima, L. C. (2015).  
367 Wind and solar hydrogen for the potential production of ammonia in the state of Ceará–Brazil. *International Journal*  
368 *of Hydrogen Energy*, 40(32), 9917-9923.
- 369 [6] Trop, P., & Goricanec, D. (2015). Comparisons between energy carriers' productions for exploiting  
370 renewable energy sources. *Energy*.
- 371 [7] Ferrero, D., Lanzini, A., Santarelli, M., & Leone, P. (2013). A comparative assessment on hydrogen  
372 production from low-and high-temperature electrolysis. *International Journal of Hydrogen Energy*, 38(9), 3523-  
373 3536.
- 374 [8] Beerbühl, S. S., Fröhling, M., & Schultmann, F. (2015). Combined scheduling and capacity planning of  
375 electricity-based ammonia production to integrate renewable energies. *European Journal of Operational*  
376 *Research*, 241(3), 851-862.
- 377 [9] Huberty, M., Schmidt, L., & Cussler, E. (2008). Small-scale Production of Renewable Ammonia. In *5th*  
378 *Ammonia Fuel Conference, Minneapolis*. Kong S.(2008). "Combustion Efficiency and Exhaust Emissions of  
379 Ammonia Combustion in Diesel Engines." *Papers of the 5th Ammonia Fuel Conference, Minneapolis* (Vol. 1).
- 380 [10] Giddey, S., Badwal, S. P. S., & Kulkarni, A. (2013). Review of electrochemical ammonia production  
381 technologies and materials. *International Journal of Hydrogen Energy*, 38(34), 14576-14594.
- 382 [11] Morgan, E., Maxwell, J., & McGowan, J. (2014). Wind-powered ammonia fuel production for remote  
383 islands: A case study. *Renewable Energy*, 72, 51-61.

- 384 [12] Laguna-Bercero, M. A. (2012). Recent advances in high temperature electrolysis using solid oxide fuel  
385 cells: A review. *Journal of Power Sources*, 203, 4-16.
- 386 [13] Patil, A., Laumans, L., & Vrijenhoef, H. (2014). Solar to Ammonia—Via Proton's NFuel Units. *Procedia*  
387 *Engineering*, 83, 322-327.
- 388 [14] O'Brien, J. E., McKellar, M. G., Harvego, E. A., & Stoots, C. M. (2010). High-temperature electrolysis for  
389 large-scale hydrogen and syngas production from nuclear energy—summary of system simulation and economic  
390 analyses. *International Journal of Hydrogen Energy*, 35(10), 4808-4819.
- 391 [15] Dybkjaer, I. (1995). Ammonia production processes. In *Ammonia* (pp. 199-327). Springer Berlin  
392 Heidelberg.
- 393 [16] Max Appl. (1999). *Ammonia: principles and industrial practice*. Vch Verlagsgesellschaft Mbh.
- 394 [17] Penchini, D., Cinti, G., Discepoli, G., & Desideri, U. (2014). Theoretical study and performance evaluation  
395 of hydrogen production by 200 W solid oxide electrolyzer stack. *International Journal of Hydrogen Energy*, 39(17),  
396 9457-9466.
- 397 [18] Mondal, P., Dang, G. S., & Garg, M. O. (2011). Syngas production through gasification and cleanup for  
398 downstream applications—Recent developments. *Fuel Processing Technology*, 92(8), 1395-1410.
- 399 [19] [http://www.fch.europa.eu/sites/default/files/study%20electrolyser\\_0-Logos\\_0\\_0.pdf](http://www.fch.europa.eu/sites/default/files/study%20electrolyser_0-Logos_0_0.pdf) (last access  
400 18/03/2016)
- 401 [20] Ivanova, S., & Lewis, R. (2012). Producing Nitrogen via Pressure Swing Adsorption. *Chemical Engineering*  
402 *Progress*, 108(6), 38-42.
- 403 [21] Cinti, G., Discepoli, G., Bidini, G., Lanzini, A., & Santarelli, M. (2015). Co-electrolysis of water and CO<sub>2</sub> in  
404 a solid oxide electrolyzer (SOE) stack. *International Journal of Energy Research*, 40(2), 207-215.
- 405 [22] Frigo, S., Gentili, R. (2013) Analysis of the behaviour of a 4-stroke Si engine fuelled with ammonia and  
406 hydrogen. *International Journal of Hydrogen Energy*, 38 (3), 1607-1615.
- 407 [23] Comotti, M., Frigo, S. (2015). Hydrogen generation system for ammonia-hydrogen fuelled internal  
408 combustion engines. *International Journal of Hydrogen Energy*, 40 (33), 10673-10686
- 409